

# Double Layer Patch Resonator

Humberto César Chaves Fernandes and Rogério Torres Carvalho Filho

Department of Electrical Engineering - Technological Center - Federal University of Rio Grande do Norte, Natal RN, Brazil

**Abstract** — The theory and numeric results of the Double Layer Patch Resonator (DLPR) about resonant frequency, efficiency and bandwidth are presented. The full wave Transversal Transmission Line (TTL) method has been used for analysis. Starting from the Maxwell equations, a system that represents the electromagnetic fields are obtained, according with this concise and efficient procedures, to calculate the complex resonant frequency. This resonant frequency is calculated through double spectral variables. The new results are good and are in accordance with that results presented in the specialized literature.

## I. INTRODUCTION

The double layer patch resonator consists of one rectangular patch, with length  $l$  and width  $w$ , and three dielectrics regions, as shown in the Fig. 1. The analysis in the structure has been analyzed with the concise full wave transverse transmission line (TTL) method. This method is obtained of the electromagnetic fields general equations. In this work was obtained a form to calculate the resonant frequency of the double layer patch resonator.

This method was presented last year for single layer patch resonator [1-4]. The results were obtained in agreement with results researched in the literature. Computational simulations have been accomplished to analyze the behavior of resonators of double layer patch resonator. In the first part of this work, is used substrates with the same constant dielectric, and the results obtained are identical those with the single layer patch resonator. In the second part, the dielectric constant is changed and are presented new values of efficiency and bandwidth for variations of the resonant frequency.

An advantage in the use of double layers, for example, is to obtain one better flexibility and control of the calculated parameters, being a great option to be utilized in applications to smart and adaptative antenna array and others structures with different resonant patch [5]-[7].

## II. FIELDS IN THE STRUCTURE

Due the double layer patch resonator to have length  $l$  and width  $w$ , the equations used for the analysis in the spectral domain, are the directions "x" and "z". Therefore it is applied to the field equations the double Fourier transformed domain defined as:

H. C. C. Fernandes and R.T.C. Filho, Department of Electrical Engineering - Technological Center - Federal University of Rio Grande do Norte - UFRN - P.O.Box: 1583 - 59.072-970 Natal, RN, Brazil. - Phone: +55 (021) 84 215.3731. E-mails: [humbeccf@ct.ufrn.br](mailto:humbeccf@ct.ufrn.br); [rtcfilho@ig.com.br](mailto:rtcfilho@ig.com.br). This work received financial support by CNPq.

$$\tilde{f}(\alpha_n, y, \beta_k) = \int_{-\infty}^{\infty} \int_{-\infty}^{\infty} f(x, y, z) \cdot e^{j\alpha_n x} \cdot e^{j\beta_k z} dx dz \quad (1)$$

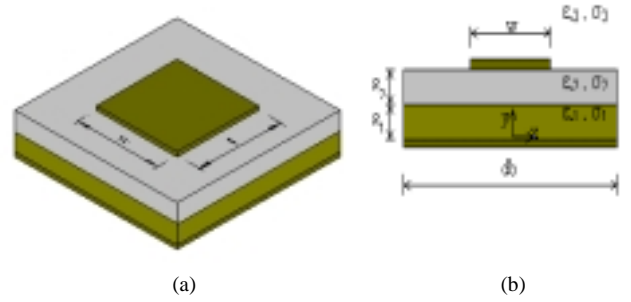


Fig. 1 – (a) Spatial view of the double layer patch resonator, and (b) It transverse section.

After using the equations of Maxwell, the general equations of the fields in the TTL method, are obtained as:

$$\tilde{E}_{xi} = \frac{1}{\gamma^2 + k_i^2} \left[ -j\alpha_n \frac{\partial}{\partial y} \tilde{E}_{yi} + \omega \mu \beta_k \tilde{H}_{yi} \right] \quad (2.1)$$

$$\tilde{E}_{zi} = \frac{1}{\gamma^2 + k_i^2} \left[ -j\beta_k \frac{\partial}{\partial y} \tilde{E}_{yi} - \omega \mu \alpha_n \tilde{H}_{yi} \right] \quad (2.2)$$

$$\tilde{H}_{xi} = \frac{1}{\gamma^2 + k_i^2} \left[ -j\alpha_n \frac{\partial}{\partial y} \tilde{H}_{yi} - \omega \epsilon \beta_k \tilde{E}_{yi} \right] \quad (2.3)$$

$$\tilde{H}_{zi} = \frac{1}{\gamma^2 + k_i^2} \left[ -j\beta_k \frac{\partial}{\partial y} \tilde{H}_{yi} + \omega \epsilon \alpha_n \tilde{E}_{yi} \right] \quad (2.4)$$

where,

$i = 1, 2, 3$ , represent the three dielectrics regions of the structure;

$$\gamma_i^2 = \alpha_n^2 + \beta_k^2 - k_i^2 \quad (2.5)$$

is the propagation constant in y direction;  $\alpha_n$  is the spectral variable in "x" direction and  $\beta_k$  is the spectral variable in "z" direction.

$k_i^2 = \omega^2 \mu \epsilon = k_0^2 \epsilon_{ri}^*$  is the wave number of the  $i^{\text{th}}$  dielectric region;

$\epsilon_{ri}^* = \epsilon_{ri} - j \frac{\sigma_i}{\omega \epsilon_0}$  is the relative dielectric constant of

the material with losses;  $\omega = \omega_r + j\omega_i$  is the complex angular frequency;

$\varepsilon_i = \varepsilon_{ri}^* \cdot \varepsilon_0$  is the dielectric constant of the material;

$\varepsilon_0$  is the free space dielectric constant;

$\sigma_i$  is the conductivity and  $\mu$  is the permeability.

The equations above are applied to the resonator being calculated, the fields  $E_y$  and  $H_y$  through the solution of the wave equations of Helmholtz in the spectral domain [2]-[3]:

$$\left( \frac{\partial^2}{\partial y^2} - \gamma^2 \right) \tilde{E}_y = 0 \quad (3.1)$$

$$\left( \frac{\partial^2}{\partial y^2} - \gamma^2 \right) \tilde{H}_y = 0 \quad (3.2)$$

The solutions of those equations for the three regions of the structure are given for:

region 1:

$$\tilde{E}_{y1} = A_{1e} \cdot \cosh \gamma_1 y \quad (4.1)$$

$$\tilde{H}_{y1} = A_{1h} \cdot \sinh \gamma_1 y \quad (4.2)$$

region 2:

$$\tilde{E}_{y2} = A_{2e} \cdot \sinh \gamma_2 y + B_{2e} \cdot \cosh \gamma_2 y \quad (4.3)$$

$$\tilde{H}_{y2} = A_{2h} \cdot \sinh \gamma_2 y + B_{2h} \cdot \cosh \gamma_2 y \quad (4.4)$$

region 3:

$$\tilde{E}_{y3} = A_{3e} \cdot e^{-\gamma_3 y} \quad (4.5)$$

$$\tilde{H}_{y3} = A_{3h} \cdot e^{-\gamma_3 y} \quad (4.6)$$

Substituting these solutions in the equations of the fields (2.1) to (2.4), as functions of the unknown constants  $A_{1e}$ ,  $A_{1h}$ ,  $B_{2e}$  and  $B_{2h}$  is obtained, for example for the region 2:

$$\tilde{E}_{x2} = \frac{-j}{\gamma_2^2 + k_2^2} [(\alpha_n \gamma_2 A_{2e} + j\beta_k \omega \mu B_{2h}) \cosh \gamma_2 y + (\alpha_n \gamma_2 B_{2e} + j\beta_k \omega \mu A_{2h}) \sinh \gamma_2 y] \quad (4.7)$$

$$\tilde{H}_{x2} = \frac{j}{\gamma_2^2 + k_2^2} [(-\alpha_n \gamma_2 A_{2h} + j\beta_k \omega \varepsilon_2 B_{2e}) \cosh \gamma_2 y + (-\alpha_n \gamma_2 B_{2h} + j\beta_k \omega \varepsilon_2 A_{2e}) \sinh \gamma_2 y] \quad (4.8)$$

For the determination of the unknown constants, are applied the boundary conditions for the regions 1, 2 and 3:

For the regions 1 and 2:  $y = g_1$

$$\tilde{E}_{x1} = \tilde{E}_{x2} \quad (5.1)$$

$$\tilde{E}_{z1} = \tilde{E}_{z2} \quad (5.2)$$

$$\tilde{H}_{x1} = \tilde{H}_{x2} \quad (5.3)$$

$$\tilde{H}_{z1} = \tilde{H}_{z2} \quad (5.4)$$

$$\tilde{E}_{x2} = \tilde{E}_{x3} = \tilde{E}_{xg} \quad (5.5)$$

$$\tilde{E}_{z2} = \tilde{E}_{z3} = \tilde{E}_{zg} \quad (5.6)$$

After several calculations the unknown constants "A" are obtained, for example:

$$A_{2e} = \frac{j(\alpha_n \tilde{E}_{xg} + \beta_k \tilde{E}_{zg}) \sinh \gamma_2 g_1 - (\alpha_n \tilde{E}_{xg} + \beta_k \tilde{E}_{zg}) \sinh \gamma_2 g_2}{\gamma_2 \sinh \gamma_2 g_2} \quad (6.1)$$

$$A_{2h} = \frac{(\beta_k \tilde{E}_{xg} - \alpha_n \tilde{E}_{zg}) \cosh \gamma_2 g_1 - (\beta_k \tilde{E}_{xg} - \alpha_n \tilde{E}_{zg}) \cosh \gamma_2 g_2}{\omega \mu \sinh \gamma_2 g_2} \quad (6.2)$$

Then the general equations of the electromagnetic fields in the resonator structure as function of  $\tilde{E}_{xg}$  and  $\tilde{E}_{zg}$  are obtained.

### III. ADMITANCE MATRIX

Applying the boundary conditions the following equations that relate the current densities ( $\tilde{J}_{xg}$  and  $\tilde{J}_{zg}$ ) and the magnetic fields in the interface  $y = g$ , are obtained:

$$\tilde{H}_{x2} - \tilde{H}_{x3} = \tilde{J}_{zg} \quad (7.1)$$

$$\tilde{H}_{z2} - \tilde{H}_{z3} = -\tilde{J}_{xg} \quad (7.2)$$

Being made the substitutions of the equations of the magnetic fields, given as function of ( $\tilde{E}_{xg}$  and  $\tilde{E}_{zg}$ ), and after some calculations it is obtained,

$$Y_{xx} \tilde{E}_{xg} + Y_{xz} \tilde{E}_{zg} = \tilde{J}_{zg} \quad (8.1)$$

$$Y_{zx} \tilde{E}_{xg} + Y_{zz} \tilde{E}_{zg} = \tilde{J}_{xg} \quad (8.2)$$

at the matrix form yield:

$$\begin{bmatrix} Y_{xx} & Y_{xz} \\ Y_{zx} & Y_{zz} \end{bmatrix} \begin{bmatrix} \tilde{E}_{xg} \\ \tilde{E}_{zg} \end{bmatrix} = \begin{bmatrix} \tilde{J}_{zg} \\ \tilde{J}_{xg} \end{bmatrix} \quad (9)$$

the " Y " admittances functions are the dyadic Green functions of the resonator and they are given, for example, for  $Y_{xx}$  e  $Y_{zz}$ :

$$Y_{xx} = \frac{j}{\omega \mu (\gamma_2^2 + k_2^2)} \left[ \left( \frac{-\beta_k^2 \gamma_2 d_1}{B} + \frac{k_2^2 \alpha_n^2 e_1}{A} \right) \cosh \gamma_2 g + \left( \frac{-\beta_k^2 \gamma_2 f_1}{B} + \frac{k_2^2 \alpha_n c_1}{A} \right) \sinh \gamma_2 g \right] - \frac{j(k_3^2 - \beta_k^2)}{\omega \mu \gamma_3} \quad (9.1)$$

For the regions 2 and 3:  $y = g$ ; ( $g = g_1 + g_2$ )

$$Y_{zz} = \frac{j}{\omega\mu(\gamma_2^2 + k^2)} \left[ \left( \frac{\alpha_n^2 \gamma_2 d_1}{B} - \frac{\beta_k^2 k^2 e_1}{A} \right) \cosh \gamma_2 g + \left( \frac{\gamma_2 f_1}{B} - \frac{\beta_k^2 k^2 c_1}{A} \right) \sinh \gamma_2 g \right] - \frac{j(k^2 + \alpha_n^2)}{\omega\mu\gamma_3} \quad (9.2)$$

where A and B are:

$$A = \gamma_1 \sinh \gamma_1 g_1 \cdot \cosh \gamma_2 g_2 + \gamma_2 \frac{\epsilon_1}{\epsilon_2} \cosh \gamma_1 g_1 \cdot \sinh \gamma_2 g_2 \quad (10.1)$$

$$B = \sinh \gamma_1 g_1 \cdot \cosh \gamma_2 g_2 + \frac{\gamma_1}{\gamma_2} \cosh \gamma_1 g_1 \cdot \sinh \gamma_2 g_2 \quad (10.2)$$

$$c_1 = \frac{\gamma_1}{\gamma_2} \sinh \gamma_1 g_1 \quad (10.3)$$

$$d_1 = \frac{\gamma_1}{\gamma_2} \cosh \gamma_1 g_1 \quad (10.4)$$

$$e_1 = \frac{\epsilon_1}{\epsilon_2} \cosh \gamma_1 g_1 \quad (10.5)$$

$$f_1 = \sinh \gamma_1 g_1 \quad (10.6)$$

The current densities are expanded in terms of known base functions as [3], [8]:

$$\tilde{J}_{xg} = \sum_{i=1}^n a_{xi} \cdot \tilde{f}_{xi}(\alpha_n, \beta_k) \quad (11.1)$$

$$\tilde{J}_{zg} = \sum_{j=1}^m a_{zj} \cdot \tilde{f}_{zj}(\alpha_n, \beta_k) \quad (11.2)$$

where  $a_{xi}$  and  $a_{zj}$  are constant unknown and the terms n and m are numbers integer and positive.

The base functions were chosen in the space domain, as example:

$$f_x(x, z) = f_x(x) \cdot f_x(z) \quad (12.1)$$

$$f_x(x) = \frac{1}{\sqrt{\left(\frac{w}{2}\right)^2 - x^2}} \quad (12.2)$$

$$f_x(z) = \cos\left(\frac{\pi z}{l}\right) \quad (12.3)$$

whose Fourier transformed are:

$$\tilde{f}_x(\alpha_n) = \pi \cdot J_0\left(\alpha_n \frac{w}{2}\right) \quad (13.1)$$

$$\tilde{f}_x(\beta_k) = \frac{2\pi l \cdot \cos\left(\frac{\beta_k l}{2}\right)}{\pi^2 - (\beta_k l)^2} \quad (13.2)$$

$$\tilde{f}_x(\alpha_n, \beta_k) = \frac{2\pi^2 l \cdot \cos\left(\frac{\beta_k l}{2}\right)}{\pi^2 - (\beta_k l)^2} \cdot J_0\left(\alpha_n \frac{w}{2}\right) \quad (13.3)$$

where  $J_0$  is the Bessel function of first specie and zero order.

The Galerkin method is applied to (9), to eliminate the electromagnetic fields. The new equation in matrix form is obtained,

$$\begin{bmatrix} K_{xx} & K_{xz} \\ K_{zx} & K_{zz} \end{bmatrix} \cdot \begin{bmatrix} a_x \\ a_z \end{bmatrix} = \begin{bmatrix} 0 \\ 0 \end{bmatrix} \quad (14)$$

where,

$$K_{xx} = \sum_{-\infty}^{\infty} \tilde{f}_x \cdot Z_{xx} \cdot \tilde{f}_x^* \quad (14.1)$$

$$K_{xz} = \sum_{-\infty}^{\infty} \tilde{f}_z \cdot Z_{xz} \cdot \tilde{f}_x^* \quad (14.2)$$

$$K_{zx} = \sum_{-\infty}^{\infty} \tilde{f}_x \cdot Z_{zx} \cdot \tilde{f}_z^* \quad (14.3)$$

$$K_{zz} = \sum_{-\infty}^{\infty} \tilde{f}_z \cdot Z_{zz} \cdot \tilde{f}_z^* \quad (14.4)$$

The solution of the characteristic equation of the determinant of (14) supplies the resonant frequency [9]-[11].

## IV. RESULTS

Computational programs were elaborated in the FORTRAN POWER STATION and in the MATLAB languages, to obtain the numeric results in the figures presented.

In the figs. 2 and 3, the results were obtained using substrates with dielectric constant values equal to 2.22 and 9.8.

The graphic of the fig. 2 represents the efficiency at function of the resonant frequency for values of  $w=10\text{mm}$  and  $w=15\text{mm}$ . As shown, the value of efficiency increases with the increase of resonant frequency.

The graphic of the fig. 3 represents the bandwidth as function of the resonant frequency of the patch, for values of  $w=10\text{mm}$  and  $w=15\text{mm}$ . In this figure, we can observe a decrease of the bandwidth with the increase of the frequency.

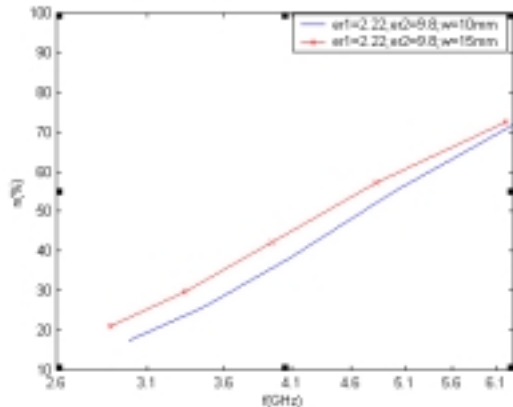


Fig. 2 – Curves of efficiency as function of the resonant frequency.

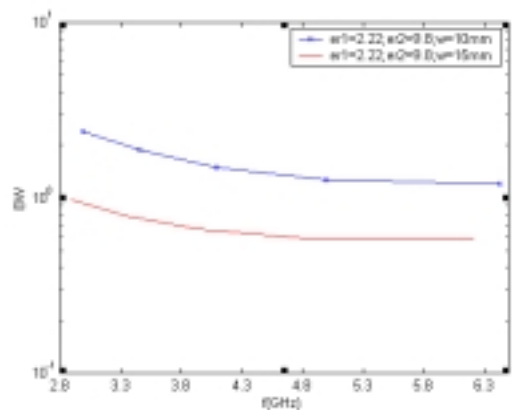


Fig.3 – Curves of bandwidth as function of the resonant frequency

The fig. 4 represents the graphic of the resonant frequency at function of the length of the patch for dielectric constant values of 2.22 and 9.8, to  $w=10\text{mm}$  and  $w=15\text{mm}$ . This graphic show that the resonant frequency decreases with the increase of the length  $l$ .

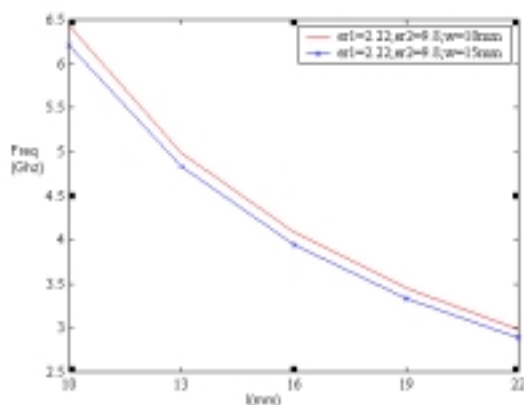


Fig.4 – Curves of resonant frequency as function of the length.

## V. CONCLUSION

The full wave method transverse transmission line (TTL) was used in the analysis for obtaining the numeric results resonant frequency, bandwidth and efficiency of the double layer patch resonator. The TTL method is an efficient and accurate method applied to the analysis, for example, for design and applications in antenna array. It is very versatile to work with lossless or semiconductor substrate. Programs computational were elaborated in the FORTRAN POWER STATION and in MATLAB languages, for obtaining of the numeric results. This work received financial support by CNPq.

## VI. REFERENCES

- [1] Humberto C. C. Fernandes, Eritônio F. Silva and Rogério T.C. Filho, "New Analysis of Superconducting Microstrip Antenna Array", IMOC2001 -SBMO/IEEE MTT-S International Microwave And Optoelectronics Conference, Belém-PA, pp.93-96, Ago. 2001.
- [2] Rogério T. C. Filho and Humberto C. C. Fernandes, "Study on Superconducting Microstrip Antenna Linear and Planar Array with TTL", 19<sup>o</sup> Brazilian Telecommunications Symposium, Fortaleza-CE, Brazil, Proc. 4 pp. CD-ROM, Sept. 2001.
- [3] Humberto C. C. Fernandes, S.A.P. Silva and L. C. de Freitas Júnior, "Coupled Superconductivity in Opened and Closed Microstrip with Various Semiconductor Substrate", 22th International Conference on Infrared and Millimeter Waves, Wintergreen, VA, USA, Conf. Proc. Pp. 343-344, 20-25 of July 1997.
- [4] S.A.P. Silva, Humberto C. C. Fernandes and L. C. de Freitas Júnior, "Complex Propagation Results in 3-D of the Generic Arbitrary Bilateral Finlines", 22th International Conference on Infrared and Millimeter Waves, Wintergreen, VA, USA, Conf. Proc. pp.340-341, 20-25 of Jul. 1997.
- [5] A.K. Shaw and K. Naishadham, "ARMA-based time-signature estimator for analyzing resonant structures by the FDTD method", IEEE Trans. on Antennas and Propagation, Vol. 49 N<sup>o</sup> 3 , pp.327 – 339, Mar. 2001.
- [6] Wen-Shyang Chen; Chun-Kun Wu; Kin-Lu Wong , "Novel compact circularly polarized square microstrip antenna ",IEEE Trans. on Antennas and Propagation, Vol. 49 N<sup>o</sup> 3 , pp. 340 -342, Mar. 2001.
- [7] A. K. Agrawal and B. Bhat, "Resonant Characteristics and End Effects of a Slot Resonator in Unilateral Fin Line", Proc. IEEE, Vol. 72, pp. 1416-1418, Oct. 1984.
- [8] B. Baht and S. K. Koul, "Analysis, design and applications of finlines", Artech House, 1987.
- [9] Humberto C. C. Fernandes, S.A.P. Silva and L. C. de Freitas Júnior, "Coupled Superconductivity in Opened and Closed Microstrip with Various Semiconductor Substrate", 22th International Conference on Infrared and Millimeter Waves, Wintergreen, VA, USA, Conf. Proc. Pp. 343-344, 20-25 of July 1997.
- [10] Humberto C. C. Fernandes, S.A.P. Silva and L. C. de Freitas Júnior, "Microstrip Line with Superconductivity in Multilayer Semiconductor", in the 3th International Khakov Symposium on Physics and Engineering of Millimeter and Submillimeter Waves, Kharkov in Ucraina, Conf. Proc. Pp. 337-339, 15 to 17 of sept. 1998.
- [11] Igor M. Araujo, Magno C. Silva and Humberto C. C. Fernandes, "Unilateral Fin Line Resonator by the TTL Analysis", PIERS2001 – Progress in Electromagnetic Research Symposium, Osaka, Japan, guest, p. 403, July 2001.